



# Real-time measurement of photo-induced effects in 9,10-phenanthrenequinone-doped poly(methyl methacrylate) photopolymer by phase-modulated ellipsometry

Chun-I. Chuang<sup>a</sup>, Yi-Nan Hsiao<sup>a</sup>, Shiuan-Huei Lin<sup>b</sup>, Yu-Faye Chao<sup>a,\*</sup>

<sup>a</sup> Department of Photonics and Institute of Electro-Optical Engineering, National Chiao Tung University, 1001 University Rd., Hsinchu 300, Taiwan, ROC

<sup>b</sup> Department of Electrophysics, National Chiao Tung University, 1001 University Rd., Hsinchu 300, Taiwan, ROC

## ARTICLE INFO

### Article history:

Received 6 November 2009

Received in revised form 14 April 2010

Accepted 16 April 2010

### Keywords:

Refractive index

Birefringence

Anisotropy axis

Photopolymer

Ellipsometry

Polarimetry

## ABSTRACT

The photo-induced effects in 9,10-phenanthrenequinone-doped (PQ-doped) poly(methyl methacrylate) (PMMA) photopolymer were studied by phase-modulated ellipsometry and polarimetry in real time. The PQ-doped PMMA was exposed to an Ar/Kr tunable laser at the wavelength of 488 nm and measured by a HeNe laser (632.8 nm). We measured the induced birefringence and the variation of the refractive index separately during exposure; there was a difference of three orders of magnitude between these two effects. This suggested that the physical mechanism of holographic recording in PQ-doped PMMA is mainly due to the photo-induced variation in the refractive index.

© 2010 Elsevier B.V. All rights reserved.

## 1. Introduction

Holographic data storage has been considered to be a promising data storage technology because it provides high storage density and fast readout rate. One of the fundamental issues for this technique to be successful is the availability of thick recording materials. Recently, research involving organic photopolymers has become of interest because of the flexibility for fabrication. Photopolymers exhibit a photo-refractive effect, and the photo-induced changes in the refractive index can be used to record the holographic interference pattern in order to form phase grating. Based on this idea, many new photopolymers have been synthesized and studied. The photo-induced refractive index variation (either due to polymerization or molecular change) and photo-induced birefringence are two of the most often used mechanisms for producing the necessary changes in refractive indices for holographic recording. Thus, various methods have been proposed for investigating these two effects in different photopolymers for further improving the properties of the recording materials. The refractive birefringence (double refraction) of photopolymers has been measured by attenuated total reflection (ATR) spectroscopy [1,2] and interferometry [3]. The refractive indices of the photopolymers have been measured by an Abbe refractometer [4] and a prism coupler [5], but the variation of the refractive index is commonly extracted from the

diffraction formula by measuring the diffraction efficiency of a recorded grating [6–8]. Recently, different configurations of ellipsometry have been used to measure the refractive index and the magnitude of birefringence of photopolymers [9–11]. Most of these methods either use the measurements from the ellipsometer to confirm their results or measure the refractive index at two static states, i.e., before and after the photo illumination. Although, it is very important to understand the sensitivity of the recording processes, a few studies have been conducted to measure the dynamics of refractive index changes during illumination, such as the dynamic measurements of photo-induced birefringence by the modified ellipsometer, which measured the phases of P-polarized and S-polarized fields separately, but simultaneously through a polarization beam splitter [12,13].

In the semiconductor industry, the *in situ* ellipsometry has been established to monitor the etching/deposition process in real time for more than a decade [14]. Since this technique is mature enough to study the ellipsometric parameters in real time, we are interested in investigating the feasibility of using phase-modulated ellipsometry (PME) to study the photo-induced dynamics of photopolymers. Hsiao et al. have fabricated a new PQ and methyl methacrylate (MMA) molecules with very low photo-induced shrinkage property (shrinkage coefficient  $\approx 10^{-5}$ ) [15] and proven that this PQ-doped PMMA can form a new type of adduct when it is exposed to light [6]. So, the photo-induced dynamics of PQ-doped PMMA can be measured by the PME without having to consider the changes in its thickness. For minimizing the temperature effect on the refractive index during exposure, we employed a low-power Ar/Kr laser (488 nm, 19 mW/cm<sup>2</sup>) to irradiate the sample. It is known that the

\* Corresponding author. Tel./fax: +886 3 5731914.

E-mail address: [yfchao@mail.nctu.edu.tw](mailto:yfchao@mail.nctu.edu.tw) (Y.-F. Chao).

temperature gradient of the refractive index of PQ-doped PMMA is  $-2.09332 \times 10^{-4} \text{ }^\circ\text{C}^{-1}$  [16]. Using two wavelengths in polarimetry for a thick medium ( $\approx 2$  mm), we were able to resolve the magnitude of birefringence ( $\Delta n$ ) better than  $10^{-6}$  [17].

## 2. Theoretical background

The photoelastic modulator (PEM) was developed to replace the compensator in ellipsometry by Jaspersen and Schnatterly [19] and later improved by Acher et al. [20]. This temporal phase-modulated ellipsometry operates under a fixed polarizer and analyzer, but measures its polarization state by the modulated phase. Because there is no mechanical moving parts in the system, beam deviation can be completely avoided, and its measuring speed is only limited by the modulation frequency. We constructed two probing systems for monitoring the photo-refractive process of a PQ-doped PMMA block under the illumination of 488 nm (Ar/Kr tunable laser): (A) PEM polarimetry for measuring the photo-induced birefringence and (B) PEM ellipsometry for measuring the refractive index changes.

### 2.1. PEM polarimetric configuration

The configuration of the phase-modulated polarimeter is shown in Fig. 1. Linearly polarized light with an azimuth angle of  $-45^\circ$  passes through the PEM. The phase of the PEM is modulated by  $\Delta_p$ , and the optic axis is at  $0^\circ$ . Then, the light is transmitted to the measured birefringent medium, the retardation of which is  $\Delta_Q$ , and its optic axis is oriented at  $\alpha$ . The phase retardation  $\Delta_p$  of the PEM is modulated as  $\delta_0 \sin \omega t$ . If the azimuth angle of the analyzer is set at  $45^\circ$ , the measured intensity can be proved to be:

$$I(\Delta_Q, \alpha) = I_0 \left[ 1 - \cos \Delta_p (\cos \Delta_Q \cos^2 2\alpha + \sin^2 2\alpha) + \sin \Delta_p \sin \Delta_Q \cos 2\alpha \right], \quad (1)$$

where  $I_0$  is the total intensity. After Fourier expansion, the intensity of Eq. (1) can be decomposed into its harmonic components [20], as shown below:

$$\begin{aligned} I_{dc} &= I_0 \\ I_{1f} &= 2I_0 J_1(\delta_0) \cos 2\alpha \sin \Delta_Q \\ I_{2f} &= -2I_0 J_2(\delta_0) (\cos \Delta_Q \cos^2 2\alpha + \sin^2 2\alpha), \end{aligned} \quad (2)$$

where  $J_i(\delta_0)$  is the  $i$ th zero-order Bessel function. We adjusted  $\delta_0$  to be 2.4065 for the convenience of setting  $J_0(\delta)$  equal to zero in the DC term. Therefore,  $\Delta_Q$  and  $\alpha$  of the birefringent medium can be obtained

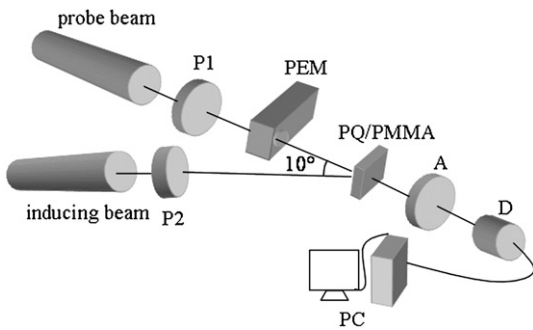


**Fig. 1.** Schematic setup of the PEM polarimeter for measuring photo-induced birefringence and its azimuth angle. Probe beam: HeNe laser (632.8 nm); inducing beam: Ar/Kr laser (488 nm); P1 and P2: polarizers; PEM: photoelastic modulator; A: analyzer; D: photodiode detector; PC: personal computer.

from the measurement of its harmonic components and deduced from the following equations:

$$\cos \Delta_Q = \frac{I_{1f}^2 J_2(\delta_0)}{2I_{dc} J_1(\delta_0)^2 [I_{2f} + 2I_{dc} J_2(\delta_0)]} - 1 \quad (3)$$

$$\sin 2\alpha = \frac{\left[ 4I_{dc}^2 - \left( \frac{I_{1f}}{J_1(\delta_0)} \right)^2 - \left( \frac{I_{2f}}{J_2(\delta_0)} \right)^2 \right]^{1/2}}{\left[ 8I_{dc}^2 - \left( \frac{I_{1f}}{J_1(\delta_0)} \right)^2 + \frac{4I_{dc} I_{2f}}{J_2(\delta_0)} \right]^{1/2}}$$

The phase retardation of the birefringent medium is:

$$\Delta_Q = \frac{2\pi \Delta n d}{\lambda} + 2m\pi, \quad (4)$$

where  $\Delta n$  is the magnitude of birefringence, and  $d$  is the thickness of the sample. The  $m$ th order ambiguity of the optical path difference has to be determined by adding an extra probe beam.

### 2.2. PEM ellipsometric configuration

In this research, we also constructed the phase-modulated ellipsometry to measure the photo-induced refractive index changes of a photo-refractive polymer during illumination. In the ellipsometric configuration (Fig. 2), the azimuth angles of the polarizer, PEM, and analyzer are set at the same values used in the polarimetric configuration, and the detected intensity [21] can be expressed as:

$$I(\Psi, \Delta) = I_0 \left[ 1 - \sin 2\Psi \cos(\Delta - \Delta_p) \right], \quad (5)$$

where  $\Psi$  and  $\Delta$  are the ellipsometric parameters of the sample, and they are related by:

$$\tan \Psi e^{i\Delta} = r_p / r_s, \quad (6)$$

where  $r_p$  and  $r_s$  represent the Fresnel complex-amplitude reflection coefficients of parallel and perpendicular components of the polarized light [22]. Using the same Fourier expansions in Eq. (5) for the modulated PEM, one can decompose the intensity into its harmonic components as:

$$\begin{aligned} I_{dc} &= 0.25I_0 [1 + \tan^2 \Psi] \\ I_{1f} &= -I_0 [\tan \Psi \sin \Delta J_1(\delta_0)] \\ I_{2f} &= -I_0 [\tan \Psi \cos \Delta J_2(\delta_0)] \end{aligned} \quad (7)$$

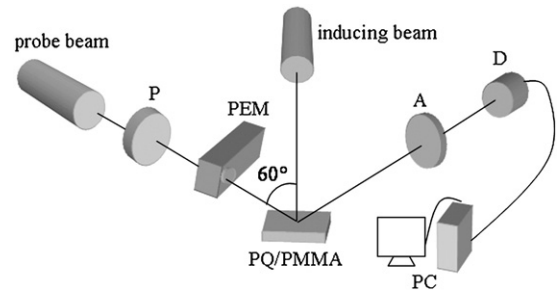


**Fig. 2.** Schematic setup of the PEM ellipsometer for measuring the variation of the refractive index of PQ-doped PMMA. Probe beam: HeNe laser (632.8 nm); inducing beam: Ar/Kr laser (488 nm); P: polarizer; PEM: photoelastic modulator; A: analyzer; D: photodiode detector; PC: personal computer.

and obtain  $\Psi$  and  $\Delta$  using the following equations:

$$\tan \Delta = \frac{I_{1f} J_2(\delta_0)}{I_{2f} J_1(\delta_0)} \quad (8)$$

$$\sin 2\Psi = \left[ \left( \frac{I_{1f}}{2I_{dc}J_1(\delta_0)} \right)^2 + \left( \frac{I_{2f}}{2I_{dc}J_2(\delta_0)} \right)^2 \right]^{1/2}.$$

For a bulk medium, the refractive index  $n_0$  of the sample can be obtained in real time by substituting the measured  $\Psi$  and  $\Delta$  into the isotropic bulk model:

$$n_0 = n_i \tan \theta_i \left[ 1 - \frac{4\rho}{(1+\rho)^2} \sin^2 \theta_i \right]^{1/2}, \quad (9)$$

where  $n_i$  is the refractive index of the ambient medium, and  $\theta_i$  is the incident angle of the probe beam [22].

### 3. Experiments

The PQ-doped PMMA probed in this research was developed by Lin's group [18]. In the probing system, the PEM (HINDS PEM-90/CF50) was used in both polarimetric and ellipsometric configurations. The strain axis of the PEM was set at  $0^\circ$ , and the azimuths of the polarizer and analyzer were positioned at  $-45^\circ$  and  $45^\circ$ , respectively, with respect to the incident plane. The modulation amplitude ( $\delta_0$ ) of PEM was calibrated [21] and adjusted to be 2.4065 for setting  $J_0(\delta)$  equal to zero in the measurements. The modulated intensities were obtained by the amplified photodetector (PDA55, Thorlabs) through the data acquisition system (PCI 6115, National Instruments). The acquired data were decomposed into harmonic signals for deducing the physical parameters of measured medium in real time; in this research, a rate of 10 sets/s can be achieved.

#### 3.1. Polarimetric configuration

Fig. 1 demonstrates the polarimetric setup. A HeNe laser at 632.8 nm with a power density of  $50 \text{ mW/cm}^2$  was used as the probe beam which transmitted through the sample; its modulated intensity can be acquired by the detection system, and the measured quantities can be displayed in real time. Instead of measuring the photo-refractive process, we first introduced a rotating quarter-wave plate (Knight Optical, RYM2504) to verify the measurements of  $\Delta_Q$  and  $\alpha$ . The entire measurement period lasted 50 s; we rotated the quarter-wave plate for 10 s at a rate of  $1^\circ/\text{s}$ . Then, the PQ-doped PMMA was irradiated by an Ar/Kr laser at a wavelength of 488 nm and a power density of  $19 \text{ mW/cm}^2$ . The induced  $\Delta_Q$  and  $\alpha$  were measured by polarimetry. The inducing beam, which was used to irradiate the sample, passed through a polarizer (P2) with the azimuth set at approximately  $30^\circ$  with an incident angle of  $10^\circ$ . For solving the ambiguity of the thickness of the sample, we turned off the inducing beam after the PQ-doped PMMA block had been fully developed and became transparent. Then, we measured the  $\Delta_Q$  and  $\alpha$  of the block by substituting the probing beam from the 632.8 nm HeNe laser to the 514 nm Ar/Kr laser.

#### 3.2. Ellipsometric configuration

The reflection coefficients were measured by PEM ellipsometry, as shown in Fig. 2. The measurements employed the probe beam at an incident angle of  $60^\circ$  on the normally induced sample. Because this incident direction is close to the Brewster angle, one can maximize the sensitivity of the measurement. Since a bulk model can be used to obtain the refractive index in real time, we specially fabricated a PQ-doped PMMA, wedge-shaped block that was 1.92 mm thick to separate the multiple reflections. In addition to measuring the refractive index of the

PQ-doped PMMA, we measured the refractive index of a pure PMMA block exposed to the same inducing beam.

### 4. Experimental results and discussion

For evaluating the measuring ability of PEM polarimetry, we first measured the  $\Delta_Q$  and  $\alpha$  of a rotating mica quarter-wave plate and displayed these values in real time on a PC monitor, as shown in Fig. 3. Before initiating the rotation, the average phase retardation and azimuth angle of the quarter-wave plate were  $91.99 \pm 0.06^\circ$  and  $9.99 \pm 0.02^\circ$ , respectively. In the end, they were stabilized to the value of  $91.84 \pm 0.06^\circ$  and  $19.99 \pm 0.02^\circ$ , respectively. The slight difference in the phase retardation was caused by the misalignment of the optical path. These results gave us enough confidence to measure the photo-induced process of the PQ-doped PMMA. For solving the ambiguity of order as described in Eq. (4), we employed two wavelengths (632.8 nm and 514 nm) to measure the phase retardation after the sample had been extensively exposed to the 488 nm line of Ar/Kr laser. At wavelengths of 632.8 nm and 514 nm, the saturated  $\Delta_Q$  values were  $115.25^\circ$  and  $115.55^\circ$ , respectively. By solving the two simultaneous equations, we determined that  $m$  was 0 and that the magnitude of the saturated birefringence  $\Delta n$  was  $7.1 \times 10^{-5}$  at 632.8 nm. The induced  $\alpha$  and  $\Delta_Q$  can be displayed on the monitor in real time, as shown in Fig. 4(a) and (b). It can be shown by Eq. (3) that the azimuth angle measured by this polarimetric model for an isotropic medium should be  $45^\circ$ . In Fig. 4, one can observe the photo-induced birefringence process of the PQ/PMMA in real time. The azimuth of the optical axis of the photo-induced birefringence started at  $43^\circ$  (close to be isotropic medium) then reached  $27.31^\circ$ , which is close to what was set for the azimuth of polarizer 2 (P2). Similar processes can be observed in the variation of retardation, i.e., the phase retardation almost started from zero (shown in Fig. 4(b)) then saturated after the sample was irradiated for 100 s; the total exposure energy was  $1.9 \text{ J/cm}^2$ . In

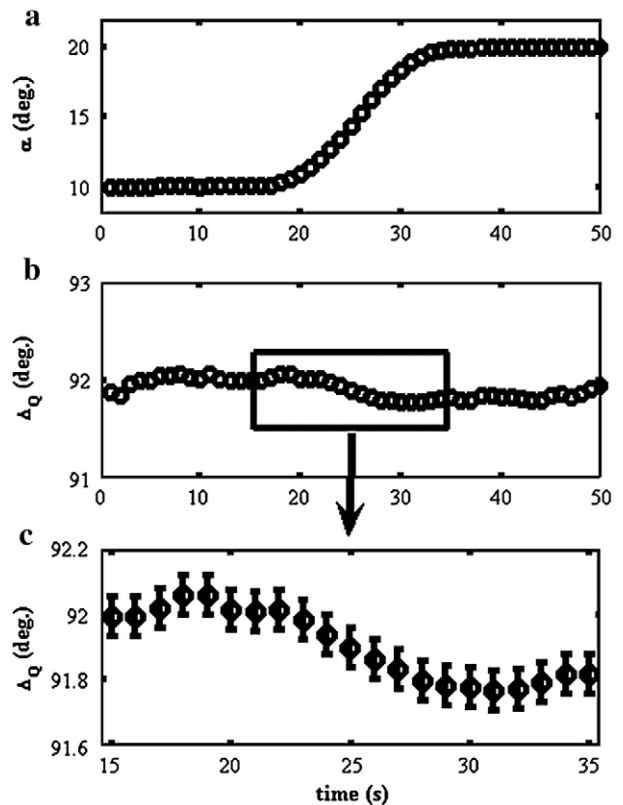
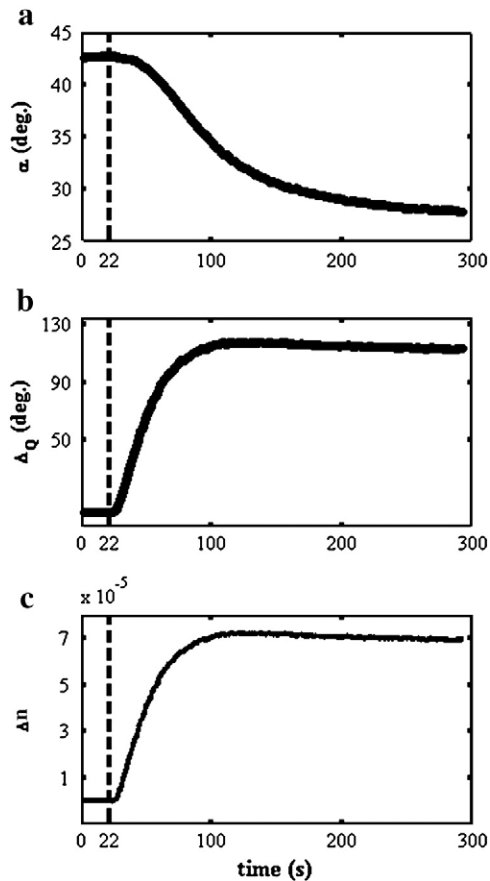


Fig. 3. (a): Azimuth angle of the optical axis; (b): phase retardation of the rotating mica quarter-wave plate; and (c): zoom-in of (b).



**Fig. 4.** (a): Azimuth angle; (b): photo-induced phase retardation; and (c): magnitude of the birefringence of PQ-doped PMMA during exposure. The 488 nm laser was turned on at the 22nd second.

addition, the magnitude of the birefringence ( $\Delta n$ ) can be calculated, and shown in Fig. 4(c).

Without using a polarizer in the inducing beam for observing the photo-refractive process, we first measured the refractive index of a 1.88 mm thick PMMA block under normal irradiation of the Ar/Kr laser at a wavelength of 488 nm from the 200th second to the 500th second. We found that the refractive index of pure PMMA was  $1.493 \pm 0.003$  and remained steady before and after irradiation, as shown in Fig. 5. This result is comparable to that in Krevelen's book on the properties of polymers [23]. This phenomenon also confirmed that PQ-doped PMMA forms a new adduct during exposure, since we observed that the refractive index of PQ-doped PMMA changed from 1.497 to 1.487 under the illumination of 488 nm wave, as shown in Fig. 6. Our results also illustrated that the rate of change in the refractive index ( $dn_0/dt$ ) started from  $-3.77 \times 10^{-6} \text{ s}^{-1}$  then reduced to  $-6.72 \times 10^{-7} \text{ s}^{-1}$  because the medium became saturated by the total exposure energy density of  $68.4 \text{ J/cm}^2$ .

Using null ellipsometry, Nee et al. measured the refractive index of a fully developed (2 h UV irradiation) PQ-doped PMMA to be 1.4899 [11], which is comparable to that of our measurement (1.487). However, the refractive index modulation measured by the Bragg diffraction angle was highly underestimated ( $3.25 \times 10^{-4}$  [6]) in comparison with that of our measurement due to the absorption and scatter losses [24,25] in the grating structure. Whether this direct measurement technique can be applied to holographic storage must be investigated further. However, compared with the results shown in Figs. 4 and 6, the photo-induced birefringence is three orders of magnitude less than the photo-induced variation in the refractive index, but its sensitivity to the total exposure energy is at least 36 times greater than that of the photo-induced variation in the refractive index.

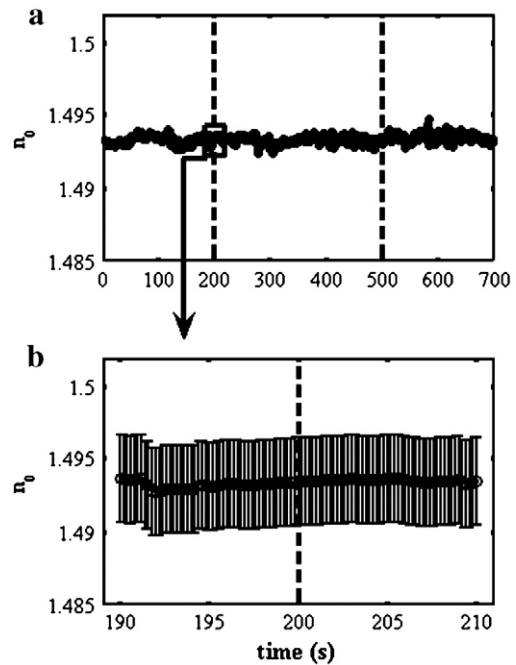


**Fig. 5.** (a): Refractive index of pure PMMA during exposure. The 488 nm laser was turned on at the 200th second and then turned off at the 500th second. The average refractive index was  $1.493 \pm 0.003$ ; and (b): zoom-in of (a).

## 5. Conclusions

The photo-induced changes in the refractive index and birefringence of PQ-doped PMMA can be measured by PEM ellipsometry and polarimetry in real time. With a total exposure energy density of  $68.4 \text{ J/cm}^2$ , the refractive index of the PQ-doped PMMA block changed from 1.497 to 1.487. In addition, at a total exposure energy density of  $1.9 \text{ J/cm}^2$ , the photo-induced birefringence was estimated to be  $7.1 \times 10^{-5}$ . The azimuth direction of the induced birefringence was identical to that of the inducing beam. From these two measurements, we can conclude that the holographic recording in PQ-doped PMMA was mainly due to the change in the refractive index. The change in the refractive index is produced by molecular structure changes of the PQ molecules because they attach to the molecules of the residual monomer, MMA [6].

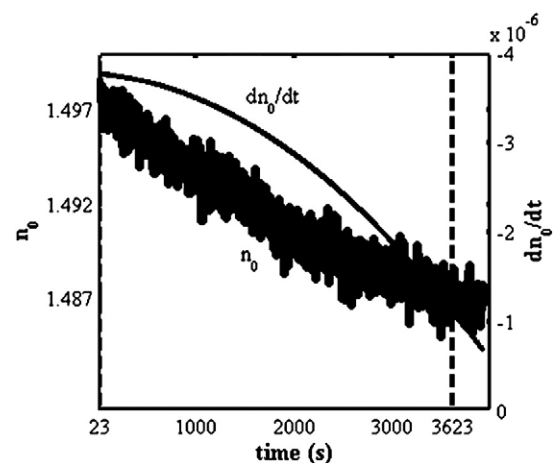


**Fig. 6.** Rate of change of the refractive index of PQ-doped PMMA during exposure; the 488 nm laser was turned on at the 23rd second and turned off at the 3623rd second.

## Acknowledgement

The authors acknowledge the funding from the National Science Council of Taiwan under the grant NSC 98-2221-E-009-024.

## References

- [1] Z. Sekkat, J. Wood, E.F. Aust, W. Knoll, W. Volksen, R.D. Miller, *J. Opt. Soc. Am. B* 13 (1996) 1713.
- [2] J.A. Delaire, K. Nakatani, *Chem. Rev.* 100 (2000) 1817.
- [3] E. Watanabe, J. Mizuno, C. Fujikawa, K. Kodate, *Proc. SPIE* 6488 (2007) 64880A-1.
- [4] S. Sainov, C. Ecoffet, D.J. Lougnot, *J. Optoelectron. Adv. M.* 7 (2005) 1311.
- [5] J.M. Yu, X.M. Tao, H.Y. Tam, *Opt. Lett.* 29 (2004) 156.
- [6] Y.N. Hsiao, W.T. Whang, S.H. Lin, *Opt. Eng.* 43 (2004) 1993.
- [7] A.I. Gusarov, D.B. Doyle, *Opt. Lett.* 25 (2000) 872.
- [8] T.G. Robinson, R.G. Decorby, J.N. McMullin, C.J. Haugen, S.O. Kasap, D. Tonchev, *Opt. Lett.* 28 (2003) 459.
- [9] J.H. Chen, D.C. Su, J.C. Su, *Appl. Phys. Lett.* 81 (2002) 1387.
- [10] O.M. Tanchak, C.J. Barrett, *Macromolecules* 38 (2005) 10566.
- [11] T.W. Nee, S.M.F. Nee, M.W. Kleinschmit, M.S. Shahriar, *J. Opt. Soc. Am. A* 21 (2004) 532.
- [12] S.G. Cloutier, D.A. Peyrot, T.V. Galstian, R.A. Lessard, *J. Opt. A Pure Appl. Opt.* 4 (2002) S228.
- [13] D. Apitz, C. Svanberg, K.G. Jespersen, T.G. Pedersen, P.M. Johansen, *J. Appl. Phys.* 94 (2003) 6263.
- [14] S.A. Hench, W.M. Duncan, L.M. Lowenstein, S.W. Butler, *J. Vac. Sci. Technol. A* 11 (1993) 1179.
- [15] S.H. Lin, J.H. Lin, P.L. Chen, Y.N. Hsiao, K.Y. Hsu, *J. Nonlinear Opt. Phys. Mater.* 15 (2006) 239.
- [16] J.M. Russo, R.K. Kostuk, *Appl. Opt.* 46 (2007) 7494.
- [17] Y.F. Chao, M.W. Wang, Z.C. Ko, *J. Phys. D Appl. Phys.* 32 (1999) 2246.
- [18] S.H. Lin, P.L. Chen, Y.N. Hsiao, W.T. Whang, *Opt. Commun.* 281 (2008) 559.
- [19] S.N. Jaspersen, S.E. Schnatterly, *Rev. Sci. Instrum.* 40 (1969) 761.
- [20] O. Acher, E. Began, B. Drevillon, *Rev. Sci. Instrum.* 60 (1989) 65.
- [21] M.W. Wang, Y.F. Chao, K.C. Leou, F.H. Tsai, T.L. Lin, S.S. Chen, Y.W. Liu, *Jpn. J. Appl. Phys.* 43 (2004) 827.
- [22] R.M.A. Azzam, N.M. Bashara, *Ellipsometry and Polarized Light*, first ed., North-Holland, Amsterdam, 1977.
- [23] D.W. Van Krevelen, K. Te Nijenhuis, *Properties of Polymers*, fourth ed., Elsevier, Amsterdam, 2009 pp. 295.
- [24] C. Neipp, I. Pascual, A. Beléndez, *J. Opt. A Pure Appl. Opt.* 3 (2001) 504.
- [25] N. Chateau, J.C. Saget, P. Chavel, *Pure Appl. Opt.* 2 (1993) 299.